

# Photon-Phonon-assisted tunneling through a single-molecular quantum dot

Bing Dong<sup>1,2</sup>, H. L. Cui<sup>1,3</sup>, and X. L. Lei<sup>2</sup>

<sup>1</sup>*Department of Physics and Engineering Physics,*

*Stevens Institute of Technology, Hoboken, New Jersey 07030*

<sup>2</sup>*Department of Physics, Shanghai Jiaotong University, 1954 Huashan Road, Shanghai 200030, China*

<sup>3</sup>*School of Optoelectronics Information Science and Technology, Yantai University, Yantai, Shandong, China*

Based on exactly mapping of a many-body electron-phonon interaction problem onto a one-body problem, we apply the well-established nonequilibrium Green function technique to solve the time-dependent phonon-assisted tunneling at low temperature through a single-molecular quantum dot connected to two leads, which is subject to a microwave irradiation field. It is found that in the presence of the electron-phonon interaction and the microwave irradiation field, the time-average transmission and the nonlinear differential conductance display additional peaks due to pure photon absorption or emission processes and photon-absorption-assisted phonon emission processes. The variation of the time-average current with frequency of the microwave irradiation field is also studied.

PACS numbers: 73.40.Gk, 73.63.Kv, 85.65.+h

## I. INTRODUCTION

The role of inelastic scattering in electron transport through mesoscopic devices is an active topic of current theoretical and experimental interest.<sup>1,2,3,4,5,6,7,8,9,10,11</sup> Thanks to the modern advanced nanostructure techniques, we can build semiconductor quantum dots (QDs) with easy control of its size and shape. Recent experiments found that the electron-phonon interaction (EPI) for longitudinal optical phonons in semiconductor QD can be substantially enhanced due to the quantum confinement effect, and also revealed the importance of the EPI in transport measurements through this kind of single electron transistor. On the other hand, a growing interest has been payed recently to electrical transport through a very small single molecular device. In contrast to the semiconductor QD, the molecular material possess much weaker elastic parameters, leading to that their internal vibration degrees of freedom is of “low-energy”, 1-10 meV.<sup>1,2,3,4</sup> Therefore, when there are electrons incident into the molecule through tunneling junction from external environment, these low-energy boson modes (phonons) can be easily excited due to the strong coupling between these modes and the molecular electronic states, and thus react inevitably back to the tunneling of electrons even at very low temperature. For example, the interesting experimental results reported in Ref. 2 demonstrated that electron transport through a single C<sub>60</sub> molecule was significantly influenced by a single vibrational mode.

This phenomena has provoked a large amount of theoretical work on the problem of tunneling through a single level with coupling to phonon modes based on the Fermi golden rule,<sup>6</sup> the kinetic equation approach,<sup>7,8</sup> and the nonequilibrium Green’s function techniques.<sup>9,10,11</sup> Naturally, both the phonon energy and the electron-phonon coupling strength are of importance to determine transport properties of these single electron transistors. Most theoretical attempts to study this transport problem so far have focused on stationary case. As far as the energy

of boson in molecule is considered to be in the region of GHz to THz, one can imagine that more rich physics could be exploited if the device is subject to a microwave (MW) irradiation field. It has been reported that the microwave spectroscopy is a possible tool to probe the energy spectrum of small quantum systems and to measure the decoherence time of the quantum states.<sup>12</sup> So the photon-assisted tunneling (PAT) could provide a new way of understanding more essence of the EPI influence on the transport properties in molecule.

The purpose of this paper is to study the time-dependent coherent transport through a single-molecular device coupled to a local dispersionless phonon mode by means of nonequilibrium Green’s function (NGF) under the adiabatic approximation.<sup>13</sup> Actually, when inelastic processes such as phonon emission and absorption are considered in the tunneling event, electron scattering becomes a many-body problem involving electrons and various excited phonon states of the system. Since the coupling between electrons and phonons is strong in the semiconductor and the single-molecular QD, the usual perturbation theory is invalid for dealing with this scattering problem, although it has been extensively exploited with enormous success to study the conventional transport in bulk material. Recently, a nonperturbative scheme has been proposed by Bonča and Trugman<sup>14</sup> for studying the small polaron of the coupled electron-phonon system described by the Holstein model<sup>15</sup> and the Su-Schrieffer-Heeger (SSH) model.<sup>16</sup> The fundamental idea of this method is to rewrite the Hamiltonian in terms of the combined electron-phonon Fock space, such can exactly map the many-body problem onto an one-body scattering problem. Later on, this method has been further applied to the topic of inelastic electron scattering in mesoscopic quantum transport in semiconductor QDs and molecular wires under the framework of the Landauer-Büttiker scattering theory.<sup>17,18</sup> In this paper, we will redirect this procedure in terms of the NGF technique and address the inelastic PAT in a molecular QD.

The rest of this work is organized as follows. In section

II, we introduce the Hamiltonian for resonant tunneling, where electrons interact with the boson fields localized on the QD or molecule. Then we describe our methodology for studying the time-dependent tunneling and computing the time-average transmission and current by means of NGF technique. In section III, we give the numerical results and discussions. We find some new features in the time-average transmission spectrum associated with the combination effects of the photon-phonon emission or absorption. Then we predict that this photon-phonon-assisted tunneling can be observed experimentally in the bias voltage-dependent differential conductance and in the microwave spectroscopy of dc current. Finally, a brief summary is presented in Sec. IV.

## II. METHOD AND FORMULATION

### A. Model and Hamiltonian

We consider the system under investigation as the simplest case: a single-site QD couples to two noninteracting reservoirs via tunneling and interacts with a dispersionless optical phonon localized in this site. It is anticipated that this is sufficient to illustrate the main physics for transport through the semiconductor QD and molecule in the presence of many boson modes. Moreover, we neglect the spin degree of freedom and any effects of electron-electron Coulomb interactions. Therefore, the Hamiltonian of this system can be split into three parts, (1) the two isolated leads  $H_{\text{lead}}$ , (2) the single-site QD  $H_{\text{QD}}$ , and (3) the tunneling part  $H_{\text{tl}}$ :

$$H_{\text{lead}} = \sum_{\eta, k} \epsilon_{\eta k}(t) c_{\eta k}^\dagger c_{\eta k}, \quad (1a)$$

$$H_{\text{QD}} = \epsilon_d(t) c_d^\dagger c_d + \hbar\omega_{ph} b^\dagger b - \lambda c_d^\dagger c_d (b + b^\dagger), \quad (1b)$$

$$H_{\text{tl}} = \sum_{\eta, k} V_\eta (c_{\eta k}^\dagger c_d + \text{H.c.}) \quad (1c)$$

$c_{\eta k}^\dagger$  ( $c_{\eta k}$ ),  $c_d^\dagger$  ( $c_d$ ) are the creation (annihilation) operators for the noninteracting electrons with momentum  $k$  in the  $\eta$  ( $= L/R$ ) lead, and for the electronic state at the single-site, respectively. The role of the MW fields irradiated on the whole system can be described by a rigid shift of the single-electron energy spectrum under the adiabatic approximation:<sup>13</sup>  $\epsilon_{\eta k}(t) = \epsilon_{\eta k}^0 + v_{\eta}(t)$  ( $\eta = L, R$ ) and  $\epsilon_d(t) = \epsilon_d + v_d(t)$ ,  $\epsilon_{\eta k}^0$  and  $\epsilon_d$  are the time-independent single electron energy without MW fields,  $v_{\eta/d}(t)$  is the time-dependent part,  $v_{\eta/d}(t) = v_{\eta/d} \cos \Omega t$ , with  $v_{\eta/d}$  being the irradiation strength in different elements of the device and  $\Omega$  being the frequency of the MW field.  $\hbar\omega_{ph}$  is the energy of the dispersionless phonon mode and  $\lambda$  is the on-site EPI constant. In the present work, we neglect the direct coupling between the MW field and the boson field.  $V_\eta$  stands for the tunneling coupling between the dot and  $\eta$ th lead.

Obviously, this problem described by the above Hamiltonian (1) is a many-body problem involving the phonon emission and absorption when the electron tunnels through the central region. Following the pioneer work of Bonča and Trugman, we can expand the electron states in the single-site onto the polaron eigenstates, the direct-product states of the single-electron states and the phonon Fock states,

$$|0, n\rangle = c_d^\dagger \frac{(b^\dagger)^n}{\sqrt{n!}} |0\rangle, \quad (n \geq 0) \quad (2)$$

which means that the electron on the site 0 is accompanied by  $n$  number of the phonon  $\hbar\omega_{ph}$  ( $|0\rangle$  is the vacuum state). After performing this representation, the many-body on-site Hamiltonian (1b) can be mapped onto an one-body one:<sup>14,17,18</sup>

$$\tilde{H}_{\text{QD}} = \sum_{n \geq 0} [(\epsilon_d + n\hbar\omega_{ph}) |0, n\rangle \langle 0, n| - \lambda \sqrt{n+1} (|0, n+1\rangle \langle 0, n| + |0, n\rangle \langle 0, n+1|)]. \quad (3)$$

Similar expansion of electron states in the two non-interacting leads with the combined space  $|\eta k, n\rangle = c_{\eta k}^\dagger \frac{(b^\dagger)^n}{\sqrt{n!}} |0\rangle$  will change the simple  $\eta$  lead Hamiltonian (1a) to a pseudo-multi-channel model labeled by the phonon quanta  $n$  with a weight factor  $P_n = (1 - e^{-\beta\omega_{ph}}) e^{-n\beta\omega_{ph}}$ , which is the statistic probability of the phonon number state  $|n\rangle$  at the finite temperature  $T$  ( $\beta = 1/k_B T$ ). Notice that the formula  $\sum_n P_n = 1$  guarantees the statistic properties of the leads unchanged (see the details in the following subsection).

Finally, the tunneling part Eq. (1c) can be also rewritten in terms of this basis set. Considering the presumption presented here that there is no exchange between electrons and phonons in the tunneling process, only hopping of the electron states are involved in the effective tunneling Hamiltonian:

$$\tilde{H}_{\text{tl}} = \sum_{\eta, k, n} V_{\eta n} (|\eta k, n\rangle \langle 0, n| + \text{H.c.}), \quad (4)$$

where  $|\eta k\rangle$  denotes the electron state with momentum  $k$  in the  $\eta$  lead. It should be noted that this presumption is rational because the high-order tunneling processes accompanied by the phonon emission and absorption are much weaker than the direct tunneling events. And in fact, inclusion of these high-order processes in the calculations is an instant task under the present theoretical framework.  $V_{\eta n}$  is the coupling between the  $n$ th pseudo-channel in the  $\eta$  lead and the QD.

We depict the many-body tunneling process after re-modeling EPI system in terms of the combined electron-phonon Fock space: An electron incident in the pseudo-channel labeled by a particular phonon number  $n$  in the left lead can transport elastically to the central region, then excites or absorbs  $m$  numbers of phonons and exits inelastically into the  $(n \pm m)$ th channels in the left and right leads; or experiences no exchange with phonon

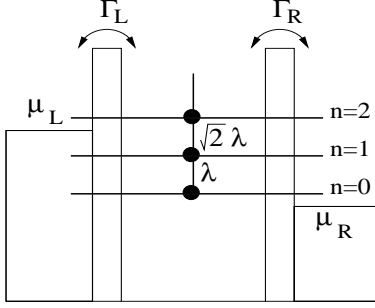


FIG. 1: Schematic description of the inelastic scattering problem for a single site with on-site EPI. Each phonon state of the site along with the Bloch state of the electron in the lead can be visualized as a pseudo-channel labeled by  $n$ , which is connected to the two leads with the hopping parameters  $\Gamma_{L/R}$  in the wide band limit. These channels are connected vertically by the EPI  $\lambda$ .

and leaves elastically at the same channel in both leads. Fig. 1 shows a graphical illustration for this description.

So far, all theoretical solutions in the literature for the phonon-assisted tunneling under above mapping Hamiltonian are based on the Landauer-Büttiker scattering formulation.<sup>14,17,18</sup> In this paper, in order to utilize the well-established NGF technique to deal with the time-dependent phonon-assisted tunneling, we first define these Dirac brackets as operators:

$$c_{dn}^\dagger = |0, n\rangle, \quad c_{\eta kn}^\dagger = |\eta k, n\rangle, \quad (5)$$

then rewrite the mapping Hamiltonian in the operator representation:

$$H_{\text{eff}} = \sum_{\eta, k, n} \epsilon_{\eta kn}(t) c_{\eta kn}^\dagger c_{\eta kn} + \sum_n [\epsilon_{dn}(t) c_{dn}^\dagger c_{dn} - \lambda \sqrt{n+1} (c_{dn+1}^\dagger c_{dn} + \text{H.c.})] + \sum_{\eta, k, n} V_{\eta n} (c_{\eta kn}^\dagger c_{dn} + \text{H.c.}), \quad (6)$$

with  $\epsilon_{\eta kn} = \epsilon_{\eta k}(t) + n\hbar\omega_{ph}$  and  $\epsilon_{dn} = \epsilon_d(t) + n\hbar\omega_{ph}$

( $n \geq 0$ ). Note that these pseudo-Fermi operators in the effective Hamiltonian are bilinear. Finally, the explicit anticommutators of these operators can be easily determined:

$$\{c_{dn}, c_{dm}^\dagger\} = \delta_{nm}, \quad \{c_{\eta kn}, c_{\eta' k' m}^\dagger\} = \delta_{\eta\eta'} \delta_{kk'} \delta_{nm}. \quad (7)$$

## B. Mathematical Formulation

In the subsection, we derive the general formula of the time-dependent transmission  $T_{\text{tot}}(t)$  and the time-average transmission  $T_{\text{tot}}$  and current  $I$  through the QD coupled to dispersionless Einstein phonons with frequency  $\omega_{ph}$  by using the NGF technique.<sup>13</sup> The time-dependent current  $J_{Ln}(t)$  from the  $n$ th channel of the left lead to the QD can be calculated from the time evolution of the occupation number operator of the electrons in this channel,  $N_{Ln} = \sum_k c_{Lkn}^\dagger c_{Lkn}$ , and one readily finds

$$J_{Ln}(t) = -e \langle \dot{N}_{Ln} \rangle = -\frac{ie}{\hbar} \langle [H_{\text{eff}}(t), N_{Ln}] \rangle = \frac{ie}{\hbar} \sum_k [V_{Ln} G_{n, Lkn}^<(t, t) - V_{Ln}^* \langle G_{Lkn, n}^<(t, t) \rangle]. \quad (8)$$

Here we define these hybrid retarded (advance) and lesser (greater) GFs  $G_{n, \eta km}^{r(a), <(>)}(t, t') \equiv \langle \langle c_{dn}(t) | c_{\eta km}^\dagger(t') \rangle \rangle^{r(a), <(>)}$  as follows:  $G_{n, \eta km}^{r(a)}(t, t') \equiv \pm i\theta(\pm t \mp t') \langle \{c_{dn}(t), c_{\eta km}^\dagger(t')\} \rangle$ ,  $G_{n, \eta km}^<(t, t') \equiv i \langle c_{\eta km}^\dagger(t') c_{dn}(t) \rangle$  and  $G_{n, \eta km}^>(t, t') \equiv -i \langle c_{dn}(t) c_{\eta km}^\dagger(t') \rangle$ ; and similar definitions for  $G_{\eta km, n}^{r(a), <(>)}(t, t') \equiv \langle \langle c_{\eta km}(t) | c_{dn}^\dagger(t') \rangle \rangle^{r(a), <(>)}$ . With the help of the Langreth analytic continuation rules,<sup>19</sup> these hybrid GFs can be related to the GFs of the QD  $G_{mn}^{r(a), <(>)}(t, t') \equiv \langle \langle c_{dm}(t) | c_{dn}^\dagger(t') \rangle \rangle^{r(a), <(>)}$ , where  $G_{mn}^{r(a)}(t, t') \equiv \pm i\theta(\pm t \mp t') \langle \{c_{dm}(t), c_{dn}^\dagger(t')\} \rangle$ ,  $G_{mn}^<(t, t') \equiv i \langle c_{dn}^\dagger(t') c_{dm}(t) \rangle$ , and  $G_{mn}^>(t, t') \equiv -i \langle c_{dm}(t) c_{dn}^\dagger(t') \rangle$ . Then the time-dependent current  $J_{Ln}(t)$  becomes

$$J_{Ln}(t) = \frac{e}{\hbar} |V_{Ln}|^2 \sum_k \int_{-\infty}^t dt_1 \{ G_{nn}^<(t, t_1) g_{Lkn}^a(t_1, t) + G_{nn}^r(t, t_1) g_{Lkn}^<(t_1, t) - g_{Lkn}^<(t, t_1) G_{nn}^a(t_1, t) - g_{Lkn}^r(t, t_1) G_{nn}^<(t_1, t) \}, \quad (9)$$

in which  $g_{\eta kn}^{r(a), <(>)}(t, t')$  are the free-electron GFs in the  $n$ th pseudo-channel of the  $\eta$  lead without coupling to the central region.<sup>13</sup> Employing the property  $G^r - G^a \equiv G^> - G^<$  and Noticing the definitions of these GFs, Eq. (9) can be simplified as

$$J_{Ln}(t) = \frac{e}{\hbar} |V_{Ln}|^2 \sum_k \int_{-\infty}^t dt_1 \{ G_{nn}^>(t, t_1) g_{Lkn}^<(t_1, t)$$

$$- g_{Lkn}^>(t, t_1) G_{nn}^<(t_1, t) \}. \quad (10)$$

In the wide band limit, where the hopping matrix element  $V_{\eta n} = V_\eta$  is independent on energy, one has

$$\sum_k |V_{\eta n}|^2 g_{\eta kn}^<(t, t') = i\Gamma_\eta \int \frac{d\omega}{2\pi} f_\eta^n(\omega) F(t, t'), \quad (11)$$

$$\sum_k |V_{\eta n}|^2 g_{\eta kn}^>(t, t') = -i\Gamma_\eta \int \frac{d\omega}{2\pi} [1 - f_\eta^n(\omega)] F(t, t'),$$

with  $F(t, t') = e^{-i\omega(t-t') - i \int_{t'}^t d\tau v_\eta(\tau)}$ ,  $\Gamma_\eta = 2\pi \sum_k |V_\eta|^2 \delta(\omega - \epsilon_{\eta k})$  being the generalized linewidth function, and  $f_\eta^n = \{1 + e^{(\omega + n\hbar\omega_{ph} - \mu_\eta)/k_B T}\}^{-1}$  being the Fermi distribution function of the  $n$ th pseudo-channel in the  $\eta$  lead.

Therefore to compute the time-dependent current, we have to evaluate the Keldysh GFs  $G_{nn}^{<(>)}(t, t')$ . In the following, we first calculate the retarded GF  $G_{mn}^r(t, t')$  in the equation of motion approach. Introducing the gauge transformation:<sup>20</sup>

$$G_{mn}^r(t, t') = e^{-i \int_{t'}^t d\tau v_d(\tau)} \bar{G}_{mn}^r(t, t'), \quad (12a)$$

$$G_{\eta km, n}^r(t, t') = e^{-i \int_{t'}^t d\tau v_\eta(\tau)} \bar{G}_{\eta km, n}^r(t, t'), \quad (12b)$$

one easily finds

$$\begin{aligned} & \left( i \frac{\partial}{\partial t} - \epsilon_d - m\hbar\omega_{ph} \right) \bar{G}_{mn}^r(t, t') = \delta_{mn} \delta(t - t') \\ & - \lambda \sqrt{m + 1} \bar{G}_{(m+1)n}^r(t, t') - \lambda \sqrt{m} \bar{G}_{(m-1)n}^r(t, t') \\ & + \sum_{\eta, k} V_{\eta m} \bar{G}_{\eta km, n}^r(t, t') e^{i \int_{t'}^t d\tau \Delta_\eta(\tau)}, \end{aligned} \quad (13)$$

and

$$\begin{aligned} & \left( i \frac{\partial}{\partial t} - \epsilon_{\eta k}^0 - m\hbar\omega_{ph} \right) \bar{G}_{mn}^r(t, t') = V_{\eta m}^* \bar{G}_{mn}^r(t, t') \\ & \times e^{-i \int_{t'}^t d\tau \Delta_\eta(\tau)}, \end{aligned} \quad (14)$$

with  $\Delta_\eta(t) = v_d(t) - v_\eta(t)$ . Then we transform the time coordinates to energy coordinates following the usual prescription,

$$Y(\omega, \omega') = \int dt \int dt' Y(t, t') e^{i\omega t - i\omega' t'}, \quad (15)$$

and obtain

$$\begin{aligned} & [\omega - \epsilon_d - m\hbar\omega_{ph} - \bar{\Sigma}_m^r(\omega)] \bar{G}_{mn}^r(\omega, \omega') = \delta_{mn} \delta(\omega - \omega') \\ & - \lambda \sqrt{m} \bar{G}_{(m-1)n}^r(\omega, \omega') - \lambda \sqrt{m + 1} \bar{G}_{(m+1)n}^r(\omega, \omega'), \end{aligned} \quad (16)$$

where the retarded self-energy  $\bar{\Sigma}_m^r(\omega)$  due to the coupling to the leads through the same gauge transformation as for the GFs is defined as

$$\begin{aligned} \bar{\Sigma}_m^r(\omega) &= \sum_{\eta, k} |V_{\eta m}|^2 \bar{g}_{\eta km}^r(\omega, \omega') \delta(\omega - \omega') \\ &= \sum_{\eta, k} \frac{|V_{\eta m}|^2}{\omega - \epsilon_{\eta km}^0 - m\hbar\omega_{ph} + i0^+}. \end{aligned} \quad (17)$$

In the wide band approximation, we have  $\bar{\Sigma}_m^r = -\frac{i}{2}(\Gamma_L + \Gamma_R) = -\frac{i}{2}\Gamma$ , which leads to  $\bar{\Sigma}_m^r(t, t') \rightarrow -i\frac{i}{2}\delta(t - t')$ . Here to avoid unnecessary complications, we ignore the EPI induced band narrowing, which will lead to some trivial quantitative but no significant qualitative changes for tunneling current.<sup>10</sup> Therefore, it is helpful to rewrite the resulting Eq. (16) in a compact matrix form:

$$[(\omega + i\Gamma) \mathbf{I} - \mathbf{B}] \bar{\mathbf{G}}^r(\omega) = \mathbf{I}, \quad (18)$$

in which  $\mathbf{B}$  is a  $N \times N$  ( $N = \infty$  denotes the total phonon number) symmetrical tridiagonal matrix:  $B_{nn} = \epsilon_d + (n-1)\hbar\omega_{ph}$ ,  $B_{n(n-1)} = -\lambda\sqrt{n-1}$ , and  $B_{n(n+1)} = -\lambda\sqrt{n}$ ,  $\mathbf{I}$  is the  $N$  dimensional unit matrix. A similar result is obtained for the advanced GF  $\bar{\mathbf{G}}^a(\omega)$ , and simply we have  $\bar{\mathbf{G}}^a = [\bar{\mathbf{G}}^r]^\dagger$  in the Fourier space. After performing the reverse Fourier transformation of  $\bar{\mathbf{G}}^r(\omega)$ , then substituting the resulting  $\bar{\mathbf{G}}^r(t, t')$  into Eq. (12a), one obtains

$$\mathbf{G}^r(t, t') = \int \frac{d\omega}{2\pi} \frac{1}{(\omega + i\Gamma) \mathbf{I} - \mathbf{B}} e^{-i\omega(t-t') - i \int_{t'}^t d\tau v_d(\tau)}. \quad (19)$$

Now we proceed to calculate the correlation GFs  $\mathbf{G}^{<(>)}(t, t')$ . Using the formal Keldysh GF technique, they are related to the retarded and advanced GFs as

$$\mathbf{G}^{<(>)}(t, t') = \int dt_1 \int dt_2 \mathbf{G}^r(t, t_1) \mathbf{\Sigma}^{<(>)}(t_1, t_2) \mathbf{G}^a(t_2, t'), \quad (20)$$

with the “scattering in (out)” Keldysh self-energy  $\mathbf{\Sigma}^{<(>)}$  in the matrix form with respect to the phonon number. Because the strongly correlated Hamiltonian (1) is transformed exactly to an one-body problem (6), these Keldysh self-energies are produced only by tunneling coupling to the leads and they are easily derived, in the wide band limit, as

$$\begin{aligned} \Sigma_{mn}^<(t, t') &= \sum_\eta \Sigma_{\eta m}^<(\omega) \delta(t - t') \delta_{mn} \\ &= i \sum_\eta \Gamma_\eta f_\eta^m(\omega) \delta(t - t') \delta_{mn}, \end{aligned} \quad (21a)$$

$$\begin{aligned} \Sigma_{mn}^>(t, t') &= \sum_\eta \Sigma_{\eta m}^>(\omega) \delta(t - t') \delta_{mn} \\ &= -i \sum_\eta \Gamma_\eta [1 - f_\eta^m(\omega)] \delta(t - t') \delta_{mn}. \end{aligned} \quad (21b)$$

With Eqs. (19) and (21), the Keldysh GF  $G_{mm}^{<(>)}(t, t')$  can be determined

$$\begin{aligned} G_{mm}^{<(>)}(t, t') &= \sum_{\eta, n} \int \frac{d\omega}{2\pi} e^{-i\omega(t-t') - i \int_{t'}^t d\tau v_\eta(\tau)} \\ & \times \Sigma_{\eta n}^{<(>)}/(\omega) A_{\eta mn}^r(\omega, t) [A_{\eta mn}^r(\omega, t')]^*, \end{aligned} \quad (22)$$

in terms of the the auxiliary function  $A_{\eta mn}^r(\omega, t)$ :

$$\begin{aligned} A_{\eta mn}^r(\omega, t) &= \int_{-\infty}^t dt_1 \int \frac{d\omega'}{2\pi} e^{i(\omega' - \omega)(t-t_1) - i \int_{t_1}^t d\tau \Delta_\eta(\tau)} \\ & \times \bar{G}_{mn}^r(\omega'). \end{aligned} \quad (23)$$

Finally we substitute Eqs.(11), (22) and (23) into Eq.(10) to calculate the current  $J_{Ln}(t)$ . As described in the above subsection, the current in the  $n$ th pseudo-channel of the left lead can be divided into two parts:  $J_{Ln}^{(-)}(t)$  denotes the component outgoing from the  $Ln$  channel to all pseudo-channels in both leads while  $J_{Ln}^{(+)}(t)$  means the part incoming from all pseudo-channels in both leads into this counted channel. It is obvious that the two terms bracketed in a pair of parentheses in Eq.(10) are exactly corresponding to the two different tunneling processes, and we will write them down separately in the following. After some algebra, we obtain

$$J_{Ln}^{(-)}(t) = \frac{ie}{h}\Gamma_L \sum_{\eta,l} \int d\omega f_L^n(\omega) \Sigma_{\eta l}^>(\omega) |A_{\eta nl}^r(\omega, t)|^2, \quad (24a)$$

$$J_{Ln}^{(+)}(t) = \frac{ie}{h}\Gamma_L \sum_{\eta,l} \int d\omega [1 - f_L^n(\omega)] \Sigma_{\eta l}^<(\omega) |A_{\eta nl}^r(\omega, t)|^2. \quad (24b)$$

Another important point we must emphasize is that an appropriate weight factor should be added for any components: product by the probability  $P$  belonging to the pseudo-channel electrons inject from. Therefore, the total time-dependent current flowing through the left lead is as a sum over all pseudo-channels in the left leads:

$$J(t) = \frac{e}{h}\Gamma_L \int d\omega \sum_{\eta,n,l} |A_{\eta nl}^r(\omega, t)|^2 \times \{P_n f_L^n(\omega) \Gamma_\eta [1 - f_\eta^l(\omega)] - P_l \Gamma_\eta f_\eta^l(\omega) [1 - f_L^n(\omega)]\}. \quad (25)$$

Taking into account the fact that  $\mathbf{A}_\eta^r(\omega, t)$  is a symmetric matrix, the total current  $J(t)$  is simplified as

$$J(t) = \frac{e}{h}\Gamma_L \Gamma_R \int d\omega \sum_{n,l} |A_{Rnl}^r(\omega, t)|^2 \times \{P_n f_L^n(\omega) [1 - f_R^l(\omega)] - P_l f_R^l(\omega) [1 - f_L^n(\omega)]\}. \quad (26a)$$

We can also compute only the elastic contribution to the total current by imposing the constraint of elastic tunneling  $n = l$ :

$$J_{\text{el}}(t) = \frac{e}{h}\Gamma_L \Gamma_R \int d\omega \sum_n |A_{Rnn}^r(\omega, t)|^2 P_n [f_L^n(\omega) - f_R^n(\omega)]. \quad (26b)$$

Similarly, we can define the time-dependent total transmission  $T_{\text{tot}}(\omega, t)$  and the elastic transmission  $T_{\text{el}}(\omega, t)$  as:

$$T_{\text{tot}}(\omega, t) = \Gamma_L \Gamma_R \sum_{n,l} P_n |A_{Rnl}^r(\omega, t)|^2, \quad (27a)$$

$$T_{\text{el}}(\omega, t) = \Gamma_L \Gamma_R \sum_n P_n |A_{Rnn}^r(\omega, t)|^2. \quad (27b)$$

In order to check our model and theory, we inspect the derived current and transmission probability formulae in two special cases: 1) without the MW irradiation field;

2) absence of the EPI. First if all time-varying parts in energy are zero  $v_{L/R,d} = 0$ , one has  $A_{\eta nl}^r(\omega, t) = \bar{G}_{nl}^r(\omega)$ . Then  $t_{nl}(\omega) = \Gamma_L \Gamma_R |\bar{G}_{nl}^r(\omega)|^2$  describes the transmission probability from  $n$ th channel to the  $l$ th channel according to the Lee-Fisher formulation.<sup>21</sup> The total transmission becomes  $T_{\text{tot}}(\omega) = \sum_{n,l} P(n) t_{nl}(\omega)$ , and the time-independent total current is

$$J = \frac{e}{h}\Gamma_L \Gamma_R \int d\omega \sum_{n,l} |\bar{G}_{nl}^r(\omega)|^2 \times \{P_n f_L^n(\omega) [1 - f_R^l(\omega)] - P_l f_R^l(\omega) [1 - f_L^n(\omega)]\}. \quad (28)$$

Both of them are in consistent with the previous results based on the Landauer-Büttiker formulation. Further, if there is no EPI,  $\lambda = 0$ , the matrix  $\mathbf{B}$  reduces to a diagonal matrix with the nonzero element  $B_{nn} = \epsilon_d + (n-1)\hbar\omega_{ph}$ . Easily, we obtain

$$J = J_{\text{el}} = \frac{e}{h}\Gamma_L \Gamma_R \int d\omega \sum_n \frac{1}{|\omega - \epsilon_d - n\hbar\omega_{ph} + i\Gamma|^2} \times P_n [f_L^n(\omega) - f_R^n(\omega)]. \quad (29)$$

Recalling  $\sum_n P_n = 1$ , simple algebra calculation gives

$$J = \frac{e}{h}\Gamma_L \Gamma_R \int d\omega \frac{1}{|\omega - \epsilon_d + i\Gamma|^2} [f_L(\omega) - f_R(\omega)]. \quad (30)$$

This is the famous time-independent current formula for the non-interacting resonant-level model.

We return to the photon-phonon assisted current calculation. Because the easily measured current is the dc component, we must compute the time-average current  $I = \langle J(t) \rangle$ . Define the time-average of a time-dependent object  $Y(t)$  as

$$\langle Y(t) \rangle = \lim_{t_p \rightarrow \infty} \frac{1}{t_p} \int_{-t_p/2}^{t_p/2} dt Y(t). \quad (31)$$

Of course, if  $Y(t)$  is a periodic function of time, it is sufficient to average over the period. For the harmonic time modulation interested here, the integration over  $t_1$  in the auxiliary function  $A_{\eta mn}^r(\omega, t)$  is easily to carried out:

$$A_{\eta mn}^r(\omega, t) = \exp \left[ -i \frac{\Delta_\eta}{\Omega} \sin \Omega t \right] \times \sum_{l=-\infty}^{\infty} J_l \left( \frac{\Delta_\eta}{\Omega} \right) e^{il\Omega t} \bar{G}_{mn}^r(\omega - l\Omega), \quad (32)$$

where  $J_l(x)$  is the  $l$ th order Bessel function of the first kind and  $\Delta_\eta = v_d - v_\eta$  is the difference of the intensities of the MW field on the QD and the  $\eta$  lead. Therefore, the time averaging of the current and the transmission  $T_{\text{tot}}(\omega) = \langle T_{\text{tot}}(\omega, t) \rangle$  will be

$$I = \frac{e}{h}\Gamma_L \Gamma_R \int d\omega \sum_{n,m} \sum_{l=-\infty}^{\infty} J_l^2 \left( \frac{\Delta_R}{\Omega} \right) |\bar{G}_{nm}^r(\omega - l\Omega)|^2$$

$$\times \{P_n f_L^n(\omega) [1 - f_R^m(\omega)] - P_m f_R^m(\omega) [1 - f_L^n(\omega)]\}, \quad (33)$$

and

$$T_{\text{tot}}(\omega) = \Gamma_L \Gamma_R \sum_{n,m} P_n \sum_{l=-\infty}^{\infty} J_l^2 \left( \frac{\Delta_R}{\Omega} \right) |\bar{G}_{nm}^r(\omega - l\Omega)|^2, \quad (34)$$

and two similar expressions for  $I_{\text{el}} = \langle J_{\text{el}}(t) \rangle$  and  $T_{\text{el}}(\omega) = \langle T_{\text{el}}(\omega, t) \rangle$  if setting  $n = m$ .

### III. NUMERICAL RESULTS AND DISCUSSIONS

In this section, we start to numerically study the properties of the time-average transmission and current through a single-molecular QD under MW irradiation fields, on the basis of Eqs. (33) and (34). For simplicity, in our calculation we assume the tunneling coupling between the molecular QD and the two leads to be symmetric  $\Gamma_L = \Gamma_R = \Gamma$ , and the applied MW fields to be also symmetric  $v_L = v_R = v$  and then  $\Delta_L = \Delta_R = \Delta$ . We set the phonon energy as the unit of energy throughout the rest of the paper and choose the Fermi levels of the two leads as the reference of energy  $\mu_L = \mu_R = 0$  at equilibrium condition.

A considerably wide range for the values of the phonon energy has been estimated for various mesoscopic systems in some experimental papers, from  $10 \mu\text{eV}$  to  $10 \text{ meV}$ , in addition to a very weak coupling to the leads  $\Gamma \sim 1 \mu\text{eV}$ .<sup>1,2,3,4,5</sup> In the literature, some different values for the phonon energy  $\omega_{ph}$ , EPI constant  $\lambda$ , and the tunneling constant  $\Gamma$  have been used for theoretical analysis.<sup>7,8,9,10,11,17,18</sup> In the present paper, we will particularly choose these parameters as typical values for the purpose of providing a satisfactory interpretation for the obtainable experimental results about low-temperature tunneling in the single-molecular QD. We choose  $\lambda = 0.5$ ,  $\Gamma = 0.04$ , and  $\omega_{ph} = 1$  as the unit of energy. In the following calculations, the temperature is assumed to be  $T = 0.04$ .

Worth pointing out that the present approach is an exact method to deal with the electron-phonon coupled system with arbitrary coupling strength if the maximum number of phonons  $N_{ph}$  involved in calculation is counted up to infinite. Unfortunately it is impossible in real calculation and we have to truncate this number to a finite value as long as the computation convergence is reached with any desired accuracy. The appropriate value of  $N_{ph}$  depends on the energy of the Einstein phonon mode, the EPI constant, and the temperature of the system under investigation. Concerned with these parameters in the present paper, we choose  $N_{ph} = 5$  to obtain results with higher than 1% accuracy.

#### A. Time-average transmission

First we examine the time-average transmission. In Fig. 2 we plot the total and elastic time-average transmissions as a function of the incoming electron energy  $\omega$  for the case of QD bare level  $\epsilon_d = 0$  under different MW irradiation fields: the frequency  $\Omega$  of the MW field is (b) lower than, (c) equal to, and (d) higher than the frequency of the dispersionless phonon  $\omega_{ph}$  for the case of a weak MW intensity  $\Delta/\Omega < 1$  ( $\Delta = 0.2$ ). For comparison, we also plot the results without irradiation in Fig. 2(a). The pair of numbers  $(n, m)$  located near the peaks means numbers of the phonon and photon electrons exchange with the heat bath and the MW field, respectively, when electrons tunnel through the central region. The positive (negative) of the number denotes emission (absorption) of quanta. In absence of irradiation fields, three important features can be observed with respect to the EPI: 1) The central peak of the transmission shifts from the position  $\omega = \epsilon_d$  to  $\epsilon_d - \lambda^2/\omega_{ph}$  with a slightly suppressed amplitude (smaller than 1) due to the polaron effect; 2) The positions of the side peaks corresponding to emission of  $n$  phonons are approximately given by  $\omega = \epsilon_d - \lambda^2/\omega_{ph} + n\hbar\omega_{ph}$ , meaning that the new pseudo-channel is opened and participates contribution to tunneling; 3) There are no peaks in the left side of the central peak because before tunneling there is no available phonon for absorption at low temperature. These observations are just in agreement with the previous theoretical results.<sup>9,10,17,18</sup>

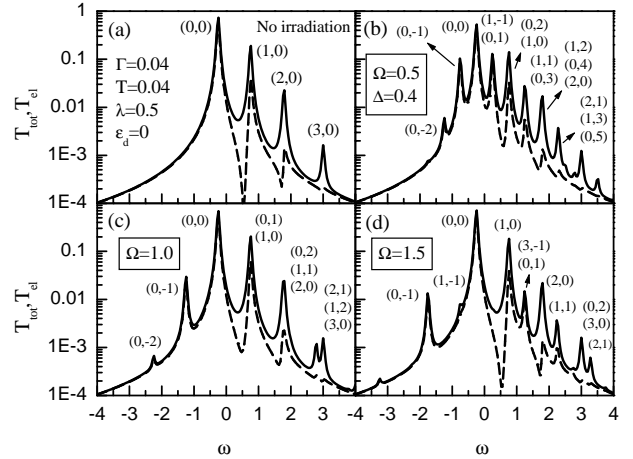


FIG. 2: Time-average transmission probability as a function of the incident electron energy under different irradiations: (a) No irradiation; (b) The frequency of the MW field  $\Omega = 0.5$ ; (c)  $\Omega = 1$ ; (d)  $\Omega = 1.5$ . The intensity of the irradiation is  $\Delta = 0.4$ . The solid line is the total transmission  $T_{\text{tot}}$ , and the dashed line is the elastic part  $T_{\text{el}}$ . The pair of numbers  $(n, m)$  near each peak denotes the numbers for emission (positive number) or absorption (negative number) of phonon and photon, respectively, involved in the tunneling process. The other parameters used in calculation are:  $\Gamma = 0.04$ ,  $\epsilon_d = 0$ ,  $\omega_{ph} = 1.0$ , and  $\lambda = 0.5$ . The temperature is set to  $T = 0.04$ .

In the presence of irradiation MW field, it is clear to observe that more rich peaks have been observed in the transmission when the involved quanta pair  $(n, m)$  satisfies  $\omega = \epsilon_d - \lambda^2/\omega_{ph} + n\hbar\omega_{ph} + m\hbar\Omega$  for the given frequency of MW field. In contrast to the phonon, pure absorption peaks of photon can be seen in negative incident energy region due to the fact that photon is independent of temperature. For the case of lower MW frequency  $\Omega = 0.5 < \omega_{ph}$  [Fig. 2(b)], there appears a new peak in the middle of the zero-phonon-peak  $(0, 0)$  and the first satellite-phonon-peak  $(1, 0)$ , which is attributed to the following two processes:  $(0, 1)$  pure emission of one-photon and  $(1, -1)$  emission of phonon assisted by absorption of one-photon. And these phonon peaks, such as  $(1, 0)$  and  $(2, 0)$ , could be also accompanied by emission of photon and photon-assisted multi-phonon processes, leading to obvious enhancement of the contribution of the elastic channel to transmission, as shown in Fig. 2(b) and (c) for the cases of irradiation fields with low frequencies. If the frequency of the MW field is higher than the frequency of phonon, no photon-assisted processes take place between the main phonon peak  $(0, 0)$  and the first phonon peak  $(1, 0)$  because there is insufficient energy to excite the high-frequency photon. As a result, the contribution of the elastic channel keeps low. More interestingly, we observe a weak emission of one-photon at the negative energy region with the help of absorption of one-photon even under this small intensity of irradiation.

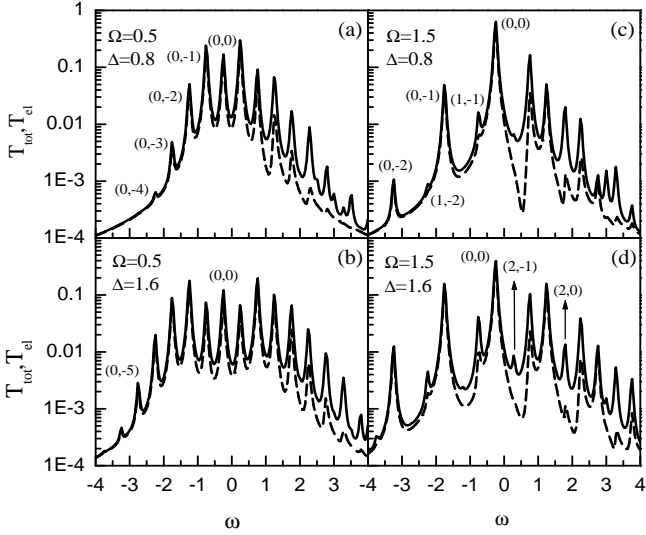


FIG. 3: Time-average transmission probability as a function of the incident electron energy under irradiations with frequencies lower [(a, b):  $\Omega = 0.5$ ] and higher [(c, d):  $\Omega = 1.5$ ] than the frequency of the Einstein phonon. The intensities of the irradiations are  $\Delta = 0.8$  (a, c) and  $1.6$  (b, d). The other parameters are the same as in Fig. 2.

Increasing intensity of the MW field will enhance the photon-assisted processes. In Fig. 3 we plot the time-average transmissions under the MW fields of frequencies  $\Omega = 0.5$  and  $1.5$  with stronger intensities  $\Delta = 0.8$  and

$1.6$ . Obviously, we observe more peaks with more high amplitudes involving emission and absorption of photons, as well as suppression of the pure phonon-assisted processes. For the strongest intensity  $\Delta = 1.6$  calculated here, the high-frequency photon ( $\Omega = 1.5$ ) even excites an emission peak involving two-phonon process between the main-phonon and the one-phonon peaks, as depicted in Fig. 3(d).

## B. Time-average current and nonlinear differential conductance

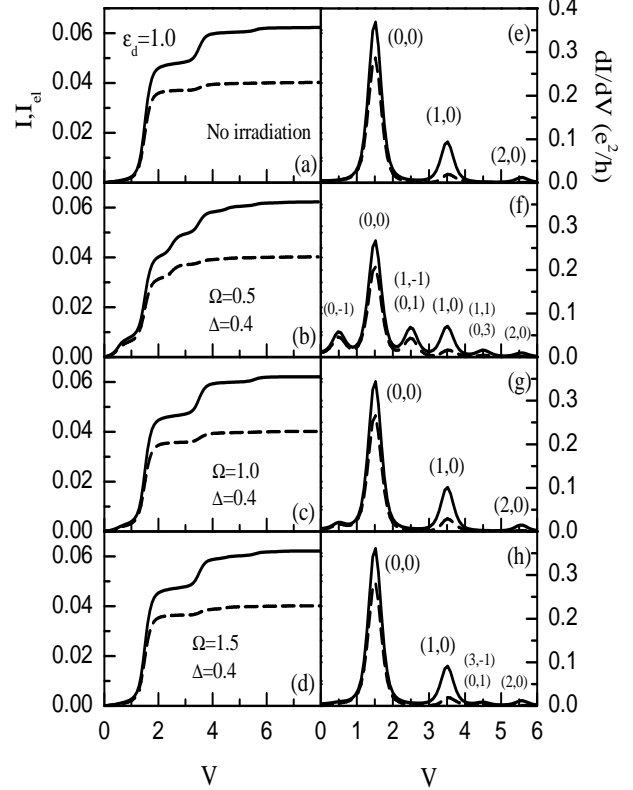


FIG. 4: The time-average total current  $I$  (solid line), elastic current  $I_{el}$  (dashed line) [(a-d)], and the corresponding differential conductance  $dI/dV$  [(e-h)] as a function of the applied bias voltage for a single-molecular QD with bare level  $\epsilon_d = 1.0$  under different irradiations: (a,e) No irradiation; (b,f) The frequency of the MW field  $\Omega = 0.5$ ; (c,g)  $\Omega = 1$ ; (d,h)  $\Omega = 1.5$ . The intensity of the irradiation is  $\Delta = 0.4$ . The other parameters are the same as in Fig. 2.

According to the current formula Eq. (33), nonlinear differential conductance, defining as the derivative of the time-average current with respect to the bias voltage  $dI/dV$  ( $dI_{el}/dV$ ), is believed to be a possible tool in experiments to detect the photon-phonon-assisted multi-peaks in time-average transmission due to its proportionality to  $T_{tot(el)}(eV)$  at low temperature. So we illustrate in Fig. 4 the calculated time-average current [(a)-(d)] and the differential conductance [(e)-(h)] for the case of bare

level  $\epsilon_d = 1.0$  without ac field (a,e) and under ac irradiations with different frequencies  $\Omega = 0.5$  (b,f), 1.0 (c,g), and 1.5 (d,h) at a weak intensity  $\Delta = 0.4$ . For simplicity, we assume the bias voltage is added symmetrically, i.e.,  $+V/2$  on the left lead and  $-V/2$  on the right lead. Obviously, the time-average current shows steps indicating that new satellite-peak in transmission denoted by  $(n, m)$  participate in conducting electrons. And correspondingly, there appears a peak in the  $dI/dV$ - $V$  curve located at the bias voltage  $eV/2 = \epsilon_d - \lambda^2/\omega_{ph} + n\hbar\omega_{ph} + m\hbar\Omega$ . For the low frequency irradiation field  $\Omega = 0.5$ , we observe a peak below the main-phonon peak  $(0, 0)$  resulted from the pure one-photon absorption process  $(0, -1)$ , which is nearly an elastic phonon process and has little inelastic contribution to the current. Moreover there is another peak between the main-phonon and the one-phonon peaks, which can be attributed to the combination contributions of a pure one-photon emission process  $(0, 1)$  and a one-photon-absorption-assisted one-phonon emission process  $(1, -1)$ . It possess of course inelastic contribution with a small portion.

As pointed above, in order to observe more photon-phonon-assisted processes, a possible method is to increase the intensity of ac field. In Fig. 5, we show the bias voltage-dependent time-average current and the differential conductance under several different microwave intensities  $\Delta = 0.4, 0.8$ , and  $1.6$  for  $\Omega = 0.5$  (a,b) and  $1.5$  (c,d). We find the following features in this figure: 1) Increasing irradiation intensity decreases the time-average current at higher bias voltage, but enhances the current at lower bias voltage; 2) The peak due to the pure phonon process  $(0, 0)$  is suppressed while the peak concerned with the photon-absorption processes  $(0, -1)$  [Fig. 5(b)] or  $(1, -1)$  [(d)] grows up gradually with rising of ac intensity; 3) These peaks due to photon-phonon combination processes have complicated relation with the ac intensity in the case of low-frequency irradiation field, which can be attributed to summation of the Bessel function with respect to the ac intensity in the time-average current formula Eq. (33).

Now we turn to study the variation of time-average current with the irradiation frequency at a given bias. Fig. 6 depicts this MW spectroscopy for the QD with bare level  $\epsilon_d = 1.0$  at a low bias voltage  $eV = 0.2$ . In this case, the low-frequency irradiation field induces a remarkable enhancement of the time-average current, in comparison with the dc current  $I_0$  without irradiation, when electrons absorb energy of photon to overcome the energy gap between the left lead and the QD. The enhanced dc current is called pumped current.<sup>22</sup> In Fig. 6, we observe two obvious peaks with one order of magnitude higher than the dc current  $I_0$ , which are due to the one-photon- and two-photon-absorption induced pumping. But the positions of the two peaks marked by triangle symbols experience blue-shift  $\Omega = (eV/2 + \lambda^2/\omega_{ph} - \epsilon_d)/m$  ( $\Omega \simeq 0.71$  for  $m = 1$ , and  $\Omega \simeq 0.35$  for  $m = 2$ ) due to the polaron effect. More interestingly, we find two more evident pumped peaks  $(1, -1)$  and  $(2, -1)$  with smaller

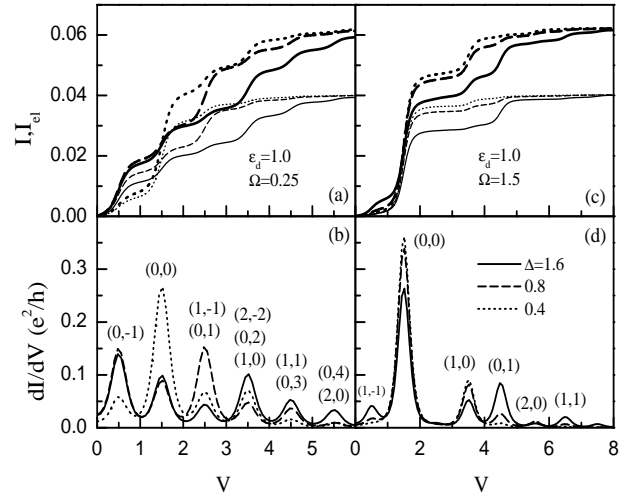


FIG. 5: The time-average current  $I$  [(a,c)], and the corresponding differential conductance  $dI/dV$  [(b,d)] vs bias voltage for the case of  $\epsilon_d = 1.0$  under several different irradiation intensities  $\Delta = 0.4$  (dotted line), 0.8 (dashed line), and 1.6 (solid line). (a,b) are plotted for  $\Omega = 0.5$ , (c,d) for  $\Omega = 1.5$ .

amplitude at high-frequency region, where the irradiation field can not only produce pumped current but also provide energy for electrons to emit phonons when electrons are pumped to tunnel through the molecule. These phonon-assisted pumped peaks locate at  $\Omega = (eV/2 + \lambda^2/\omega_{ph} - \epsilon_d - n\omega_{ph})/m$ . And they have of course higher amplitudes in the presence of stronger irradiation. This addresses that the MW spectroscopy of the pumped current is another possible method to observe the photon-phonon-assisted resonant tunneling.

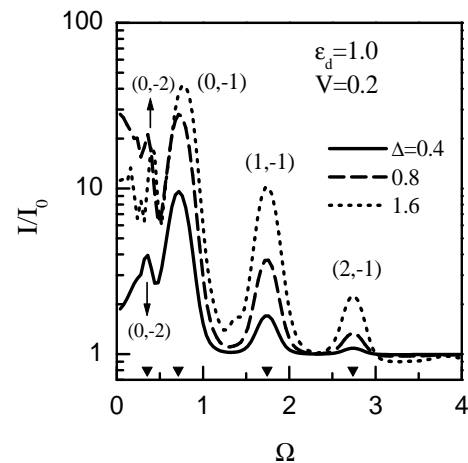


FIG. 6: The renormalized time-average total current  $I$  vs the frequency of irradiation ac field for  $\epsilon_d = 1.0$  at the bias  $eV = 0.2$  under several different irradiation intensities  $\Delta = 0.4$  (solid line), 0.8 (dashed line), and 1.6 (dotted line).  $I_0$  is the dc current of this system without irradiation.

#### IV. CONCLUSIONS

In this work we study the low-temperature time-dependent resonant tunneling through a single-molecular QD subjected to a dispersionless local phonon mode with a strong coupling to electrons. Due to the weak elastic parameters in molecular materials, the energy of boson field is matched with the MW irradiation field. So when electrons enter into the tunneling region, electrons can easily excite the phonon field with and without assistance of the ac field. Therefore, it is predicted that the combination influence of the phonon and photon fields will essentially change transport properties in the single-molecular QD.

Owing to the strong EPI, the traditional perturbation theory is invalid for this problem even though it has been intensively applied for interpretation the classic transport phenomena in bulk semiconductor. Following the pioneer work of Bonča and Trugman, we first transform this many-body problem exactly into a one-body scattering problem, by projecting the original Hamiltonian in the representation of electron-phonon coupled Fock space, i.e., the direct-product states of electron states and phonon number states. Based on this noninteracting Hamiltonian, we use the NGF approach to derive the time-dependent and the time-average transmission and

current in the wide band approximation. For the sake of simplicity, we neglect the EPI-induced band narrowing in the present calculation. Moreover we adopt the adiabatic approximation for the irradiation MW field.

Our numerical results show that time-average transmission vs incident electron energy  $\omega$  displays additional peaks, besides original phonon absorption peaks, due to photon emission or absorption mediated processes as long as the irradiation frequency matches the condition  $\omega = \epsilon_d - \lambda^2/\omega_{ph} + n\hbar\omega_{ph} + m\hbar\Omega$ . We also point out that these new features will be observed in experiments by measuring the nonlinear differential conductance and the MW spectroscopy of pumped current at proper irradiation intensity.

#### Acknowledgments

B. Dong and H. L. Cui are supported by the DURINT Program administered by the US Army Research Office. X. L. Lei is supported by Major Projects of National Natural Science Foundation of China, the Special Funds for Major State Basic Research Project (G20000683) and the Shanghai Municipal Commission of Science and Technology (03DJ14003).

---

<sup>1</sup> J. Chen, M. Reed, A. Rawlett, and J. Tour, *Science* **286**, 1550 (1999).

<sup>2</sup> H. Park, J. Park, A. Lim, E. Anderson, A. Alvisatos, and P. McEuen, *Nature* **407**, 57 (2000).

<sup>3</sup> M. Ventra, S. G. Kim, S. Pantelides, and N. Lang, *Phys. Rev. Lett.* **86**, 288 (2001).

<sup>4</sup> N. B. Zhitenev, H. Meng, and Z. Bao, *Phys. Rev. Lett.* **88**, 226801 (2002).

<sup>5</sup> T. Fujisawa, T. H. Oosterkamp, W. G. van der Wiel, B. W. Broer, R. Aguado, S. Tarucha, Leo P. Kouwenhoven, *Science* **282**, 932 (1998).

<sup>6</sup> P. J. Turley and S. W. Teitsworth, *Phys. Rev. B*, **44**, 3199 (1991).

<sup>7</sup> T. Brandes and B. Kramer, *Phys. Rev. Lett.* **83**, 3021 (1999); T. Brandes, N. Lambert, *Phys. Rev. B* **67**, 125323 (2003).

<sup>8</sup> D. Bose and H. Schoeller, *Europhys. Lett.* **54**, 668 (2001); K. D. McCarthy, N. Prokof'ev, and M. T. Tuominen, *cond-mat/0205419*; A. Mitra, I. Aleiner, and A. J. Millis, *cond-mat/0302132*, (2003).

<sup>9</sup> N. S. Wingreen, K. W. Jacobsen, and J. W. Wilkins, *Phys. Rev. Lett.* **61**, 1396 (1988); *Phys. Rev. B* **40**, 11834 (1989).

<sup>10</sup> U. Lundin and R. McKenzie, *Phys. Rev. B* **66**, 75303 (2002); J. X. Zhu and A. V. Balatsky, *Phys. Rev. B* **67**, 165326 (2003).

<sup>11</sup> K. Flensberg, *Phys. Rev. B* **68**, 205323 (2003); S. Braig and K. Flensberg, *Phys. Rev. B* **68**, 205324 (2003).

<sup>12</sup> W. G. van der Wiel, S. De Franceschi and J. M. Elzerman, T. Fujisawa, S. Tarucha, L. P. Kouwenhoven, *Rev. Modern Phys.* **75**, 1 (2003).

<sup>13</sup> A. P. Jauho, N. S. Wingreen, and Y. Meir, *Phys. Rev. B* **50**, 5528 (1994).

<sup>14</sup> J. Bonča and S. A. Trugman, *Phys. Rev. Lett.* **75**, 2566 (1995).

<sup>15</sup> T. Holstein, *Ann. Phys. (N.Y.S.)* **8**, 325 (1959).

<sup>16</sup> W. P. Su, J. R. Schrieffer, and A. J. Heeger, *Phys. Rev. Lett.* **42**, 1698 (1979).

<sup>17</sup> J. Bonča and S. A. Trugman, *Phys. Rev. Lett.* **79**, 4874 (1997); K. Haule and J. Bonča, *Phys. Rev. B* **59**, 13087 (1999).

<sup>18</sup> H. Ness and A. J. Fisher, *Phys. Rev. Lett.* **83**, 452 (1999); E. G. Emberly and G. Kirczenow, *Phys. Rev. B* **61**, 5740 (2000).

<sup>19</sup> D. C. Langreth, in *Linear and Nonlinear Electron Transport in Solids, Nato ASI, Series B* vol. 17, Ed. J. T. Devreese and V. E. Van Doren (Plenum, New York, 1976).

<sup>20</sup> T. K. Ng, *Phys. Rev. Lett.* **76**, 487 (1996).

<sup>21</sup> P. A. Lee and D. S. Fisher, *Phys. Rev. Lett.* **47**, 882 (1981).

<sup>22</sup> For review, see W. G. van der Wiel, T. H. Oosterkamp, S. De Franceschi, C. J. P. M. Harmans, and L. P. Kouwenhoven, in *Strongly Correlated Fermions and Bosons in Low-Dimensional Disordered Systems*, Ed. I. V. Lerner, B. L. Altshuler, and V. I. Fal'ko (Kluwer Academic, Dordrecht, 2002), pp. 43-68, and references therein.